IRE1α activation protects mice against acetaminophen-induced hepatotoxicity

Kyu Yeon Hur,[1] Jae-Seon So,[1] Vera Ruda,[2] Maria Frank-Kamenetsky,[3] Kevin Fitzgerald,[3] Victor Koteliansky,[3] Takao Iwawaki,[4,5,6] Laurie H. Glimcher,[1,7,8] and Ann-Hwee Lee[1,7]

[1]Deartment of Immunology and Infectious Diseases, Harvard School of Public Health, Boston, MA 02115
[2]Cardiovascular Research Center and Center for Human Genetic Research, Massachusetts General Hospital and Harvard Medical School, Boston, MA 02114
[3]Alnylam Pharmaceuticals, Cambridge, MA 02142
[4]Iwawaki Initiative Research Unit, Institute of Physical and Chemical Research, Wako, Saitama 351-0198, Japan
[5]PRESTO, Japan Science and Technology Agency, Kawaguchi, Saitama 332--0012, Japan
[6]Advanced Scientific Research Leaders Development Unit, Gunma University, Gunma 371-8511, Japan
[7]Dept of Medicine, Harvard Medical School, Boston, MA 02115
[8]Ragon Institute of MGH, MIT, and Harvard, Boston, MA 02115

The mammalian stress sensor IRE1α plays a central role in the unfolded protein, or endoplasmic reticulum (ER), stress response by activating its downstream transcription factor XBP1 via an unconventional splicing mechanism. IRE1α can also induce the degradation of a subset of mRNAs in a process termed regulated IRE1-dependent decay (RIDD). Although diverse mRNA species can be degraded by IRE1α in vitro, the pathophysiological functions of RIDD are only beginning to be explored. Acetaminophen (APAP) overdose is the most frequent cause of acute liver failure in young adults in the United States and is primarily caused by CYP1A2-, CYP2E1-, and CYP3A4-driven conversion of APAP into hepatotoxic metabolites. We demonstrate here that genetic ablation of XBP1 results in constitutive IRE1α activation in the liver, leading to RIDD of Cyp1a2 and Cyp2e1 mRNAs, reduced JNK activation, and protection of mice from APAP-induced hepatotoxicity. A pharmacological ER stress inducer that activated IRE1α suppressed the expression of Cyp1a2 and Cyp2e1 in WT, but not IRE1α-deficient mouse liver, indicating the essential role of IRE1α in the down-regulation of these mRNAs upon ER stress. Our study reveals an unexpected function of RIDD in drug metabolism.

CORRESPONDENCE
Laurie H. Glimcher:
lglimche@hsph.harvard.edu
OR
Ann-Hwee Lee:
ahlee@hsph.harvard.edu

Abbreviations used: ALT, alanine aminotransferase; APAP, acetaminophen; GSH, glutathione; JNK, c-Jun N-terminal kinase; NAPQI, N-acetyl-p-benzoquinone imine; poly(I:C), polyinosinic:polycytidylic acid; qRT-PCR, quantitative RT-PCR; RIDD, regulated IRE1-dependent decay; UPR, unfolded protein response.

The ER is an important intracellular organelle that carries out multiple physiological functions such as protein folding, posttranslational modifications, biosynthesis of fatty acids and sterols, detoxification of xenobiotics, and the storage of intracellular calcium. Hepatocytes in the liver contain abundant ER, which endows the liver with the capacity to engage in lipid and drug metabolism as well as the production of plasma proteins.

The unfolded protein response (UPR) is a signaling system that is activated when cells are exposed to agents that perturb ER protein folding homeostasis (Kaufman, 1999; Ron and Walter, 2007). IRE1α is an ER transmembrane protein that plays a major role in the initiation of the UPR both in mammals and lower eukaryotes (Cox et al., 1993; Mori et al., 1993; Wang et al., 1998; Ron and Walter, 2007). IRE1α activates the downstream transcription factor XBP1 by inducing an unconventional splicing of XBP1 mRNA, thereby generating a potent transcriptional transactivator, XBP1s (Yoshida et al., 2001; Calfon et al., 2002; Lee et al., 2002). In addition to IRE1α, two other ER transmembrane proteins, PERK and ATF6α, also constitute UPR signaling pathways in mammals (Kaufman, 1999; Ron and Walter, 2007). These three UPR signaling branches are simultaneously activated when cells are treated with chemicals that inhibit

K. Yeon Hur and J.-S. So contributed equally to this paper.

The Rockefeller University Press $30.00
J. Exp. Med. Vol. 209 No. 2 307-318
www.jem.org/cgi/doi/10.1084/jem.20111298

protein glycosylation or deplete ER calcium stores, such as tunicamycin or thapsigargin.

Analysis of mutant mice lacking key UPR regulators uncovered important physiological functions of the UPR (Lee and Glimcher, 2009; Rutkowski and Hegde, 2010). In normal cell physiology, the large amounts of proteins produced in specialized secretory cells can overwhelm ER capacity and disrupt cell homeostasis, leading to cell death, unless the ER stress is resolved by the UPR (Brewer and Hendershot, 2005). Along this line, ablation of IRE1α or XBP1 caused severe abnormalities in exocrine pancreatic acinar cells, plasma B cells, zymogenic Paneth cells, and Chief cells in the gastrointestinal tract, manifested by failure of ER expansion, reduced production of secretory proteins, and increased apoptosis (Reimold et al., 2001; Lee et al., 2005; Zhang et al., 2005; Kaser et al., 2008; Huh et al., 2010; Iwawaki et al., 2010). These studies demonstrated a critical role for the IRE1α/XBP1 UPR branch in the expansion of the cellular secretory machinery required to handle large amounts of secretory proteins.

Liver is another highly synthetic organ that produces the majority of plasma proteins. Surprisingly, however, ablation of XBP1 or IRE1α in the adult liver did not significantly decrease the plasma protein level (Lee et al., 2008; Zhang et al., 2011). Further, expression of protein secretory pathway genes was relatively normal in IRE1α- or XBP1-deficient liver unless mice were treated with a pharmacologic ER stressor, tunicamycin, which evokes a strong ER stress response (Lee et al., 2008; Zhang et al., 2011). Further, XBP1- or IRE1α-deficient hepatocytes did not exhibit any evidence of heightened ER stress, such as distended ER, reduced cell viability, or chaperone gene induction. Hence, the IRE1α–XBP1 complex does not play a major role in the protein secretory function of the adult liver under normal conditions. In contrast, ablation of XBP1 in the liver drastically reduced plasma lipid levels, uncovering a novel function of the UPR regulated by IRE1α–XBP1 in hepatic lipid metabolism (Lee et al., 2008).

We suspected, however, that this signaling pathway might have other key functions in liver, an organ responsible for the metabolism of most xenobiotics. The ER is an important organelle in drug metabolism, as most phase I enzymes including cytochrome P450 oxidases and some phase II enzymes localize to the ER (Cribb et al., 2005). Acetaminophen (APAP) is a widely used analgesic drug. Although safe at therapeutic doses, overdose of APAP can cause severe liver damage characterized by centrilobular hepatic necrosis (Mitchell et al., 1973a). APAP hepatotoxicity is mainly mediated by N-acetyl-p-benzoquinone imine (NAPQI), which is generated by oxidation of APAP by P450 enzymes such as Cyp1a2, Cyp2e1, and Cyp3a4 (Raucy et al., 1989; Patten et al., 1993; Thummel et al., 1993; Zaher et al., 1998; James et al., 2003). Cyp2e1-null mice are markedly resistant (Lee et al., 1996), whereas Cyp1a2 and Cyp2e1 double-null mice are almost completely resistant to APAP-induced hepatotoxicity (Zaher et al., 1998), indicating the essential role of these P450 enzymes in APAP induced liver damage. NAPQI is detoxified primarily by glutathione (GSH) conjugation (Mitchell et al., 1973b). However, excessive amounts of NAPQI deplete cellular GSH stores and covalently bind to macromolecules, resulting in cytotoxicity (Cohen and Khairallah, 1997). In addition, recent studies identified c-jun N-terminal kinase (JNK) as a central mediator of APAP hepatotoxicity (Gunawan et al., 2006; Henderson et al., 2007). It has been shown that NAPQI induces oxidative stress, which then activates JNK to induce cell death (Hanawa et al., 2008; Nakagawa et al., 2008).

In this study, we demonstrate that XBP1-deficient mice are protected from APAP hepatotoxicity. Ablation of XBP1 in the liver suppressed the expression of Cyp1a2 and Cyp2e1, which is critical for the conversion of APAP to the toxic NAPQI in rodents. We demonstrate that IRE1α is hyperactivated in XBP1-deficient mouse liver and cleaves Cyp1a2 and Cyp2e1mRNAs, leading to their degradation. Our study reveals a novel function of the IRE1α–XBP1 signaling pathway in drug metabolism in the liver.

RESULTS

XBP1 deficiency in the liver protects mice from APAP-induced hepatotoxicity

To investigate the function of the UPR regulated by IRE1α and XBP1 in APAP metabolism and hepatotoxicity, we used mice in which Xbp1 is inducibly deleted in the liver by polyinosinic:polycytidylic acid (poly[I:C]) treatment (Lee et al., 2008). $Xbp1^{f/f}$;Mxcre (Xbp1Δ) and the littermate control $Xbp1^{f/f}$ (WT) mice were injected with poly(I:C) and used for experiments after more than 3 wk of acclimation. A single dose of 500 mg APAP/kg markedly increased serum alanine aminotransferase (ALT) levels in WT mice, peaking at 24 h, and then decreasing to near basal levels on day 3, indicating APAP-induced acute liver injury (Fig. 1 A). In contrast, Xbp1Δ mice displayed only a modest induction of serum ALT levels by APAP treatment. APAP-induced mortality was also dramatically decreased in Xbp1Δ mice (Fig. 1 B). Histological analysis of the liver revealed markedly reduced liver injury in Xbp1Δ mice compared with WT animals that exhibited severe centrilobular necrosis and hemorrhage (Fig. 1 C), demonstrating that Xbp1 deficiency protected mice from APAP-induced hepatotoxicity.

Although the generation of toxic metabolites by hepatocytes is the primary mechanism of liver injury from APAP overdose, inflammatory responses mediated by the innate immune system also contribute to APAP hepatotoxicity (Blazka et al., 1995; Liu et al., 2004; Liu and Kaplowitz, 2006). $Xbp1^{f/f}$;Mxcre mice expressed cre recombinase both in the liver and the hematopoietic cells in the bone marrow of upon poly (I:C) injection (Martinon et al., 2010). We recently demonstrated that XBP1 is required for optimal cytokine expression in macrophages and controls the inflammatory response (Martinon et al., 2010). To ascertain that XBP1 deficiency in hepatocytes and not in innate immune cells protected mice from APAP-induced hepatotoxicity, we crossed $Xbp1^{f/f}$ mice with Alb-cre mice expressing Cre recombinase under the control of the mouse albumin promoter to achieve hepatocyte-specific deletion of XBP1 (Postic et al., 1999). Similar to Xbp1Δ

mice that lacked XBP1 both in the liver and hematopoietic cells, Xbp1$^{f/f}$;Alb-cre (Xbp1^{LKO}) mice were viable and grossly normal. Xbp1^{LKO} mice were also resistant to APAP-induced hepatotoxicity, as indicated by lower serum ALT levels and decreased necrosis compared with littermate controls (Fig. 2). These results indicate that XBP1 deficiency in liver parenchymal cells is sufficient to protect mice against APAP-induced hepatotoxicity.

Decreased expression of Cyp1a2 and Cyp2e1 in XBP1-deficient liver

To investigate the mechanism by which XBP1 regulates APAP metabolism, we measured mRNA levels of genes involved in drug metabolism using the RT^2 Profiler PCR Array (SABiosciences). Notably, Cyp1a2 and Cyp2e1, which are crucial for APAP oxidation to the toxic NAPQI, were significantly decreased in the liver of Xbp1Δ mice (Table S1). Cyp2e1 plays a major role in the conversion of APAP into hepatotoxic NAPQI (Gonzalez, 2007). Cyp1a2 also contributes to APAP metabolism and hepatotoxicity, although it has a lower APAP affinity than Cyp2e1 (Raucy et al., 1989; Patten et al., 1993). Quantitative RT-PCR (qRT-PCR) confirmed the decrease of hepatic Cyp1a2 and Cyp2e1 mRNA levels by poly(I:C) administration in Xbp1$^{f/f}$;Mxcre mice that ablated XBP1, but not in the control Xbp1$^{f/f}$ mice (Fig. 3 A). Western blotting and qRT-PCR demonstrated decreased expression of Cyp1a2 and Cyp2e1 in the liver of Xbp1^{LKO} mice as well (Fig. 3, B and C). In contrast, genes involved in GSH synthesis, such as GSH synthetase, glutamate-cysteine ligase catalytic, and glutamate-cysteine ligase modifier subunits, were unaffected by XBP1 deficiency (Fig. 3 D). Nuclear factor erythroid-2–related factor 2 (Nrf2) which is considered a key regulator of the antioxidant response (Chan and Kan, 1999; Chan et al., 2001), and its target genes such as *GSH-S-transferase pi 1* (*Gstpi*) and *UDP-glucuronosyltransferase 1a6* (*Ugt1a6*), were also unchanged in Xbp1Δ liver (Fig. 3, D and E). Collectively, these data indicate that XBP1 is required for the expression of Cyp1a2 and Cyp2e1, which are responsible for the generation of reactive NAPQI from APAP.

Effects of XBP1 ablation on APAP-induced GSH depletion and JNK activation

The reactive metabolite NAPQI generated from APAP by Cyp1a2 and Cyp2e1 P450 enzymes is normally removed by conjugation with GSH (James et al., 2003). Toxic doses of APAP deplete hepatic GSH, allowing covalent binding of NAPQI to intracellular macromolecules, which leads to cell death (Cohen and Khairallah, 1997). Hepatic GSH stores were rapidly decreased by APAP administration in both WT and Xbp1^{LKO} mice, reaching background levels within 2 h, indicating that the reactive NAPQI overwhelmed the GSH-mediated

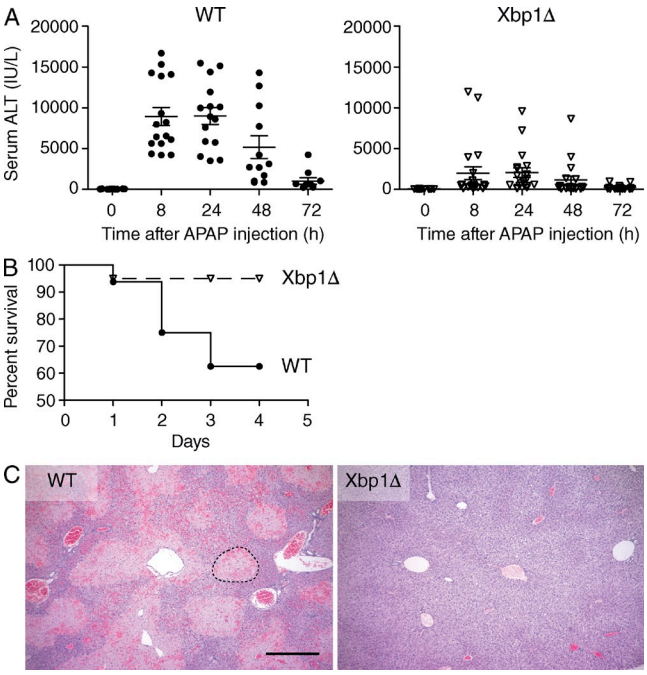

Figure 1. XBP1-deficient mice are resistant to APAP-induced liver toxicity. (A) Mice were i.p. injected with 500 mg/kg APAP after a 16-h fast. Serum ALT levels were measured at various time points. ALT measurements were performed on animals only when they were alive. Each symbol represents one mouse. Horizontal lines represent mean values and SEM. (B) Survival of WT (n = 20) and Xbp1Δ mice (n = 16) after APAP administration. $P < 0.02$ (Mantel–Cox test). (C) H&E staining of liver sections. Mice were sacrificed 24 h after APAP injection. Dotted line indicates a necrotic area. Images are representative of at least five independent experiments. Bars, 0.5 mm.

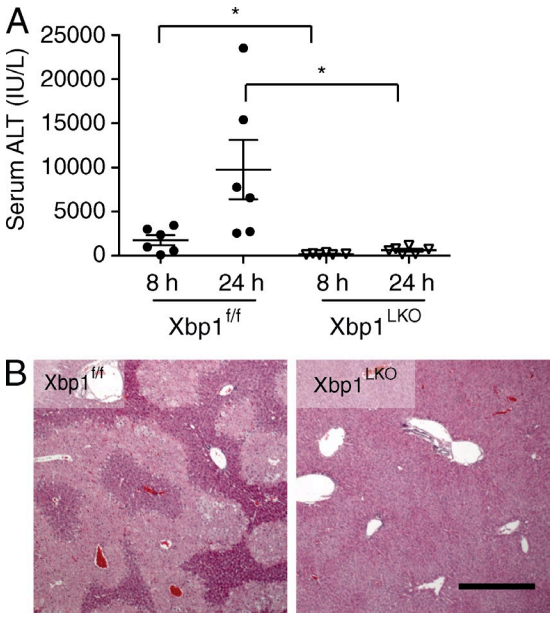

Figure 2. Protection of mice with liver-specific deletion of XBP1 (Xbp1^{LKO}) from APAP hepatotoxicity. (A) Mice were i.p. injected with 500 mg/kg APAP after a 16-h fast. Bloods were drawn via tail vein at 8 and 24 h after APAP injection for ALT measurements. *, $P < 0.05$. Horizontal lines represent mean values and SEM. (B) H&E staining of liver sections. Mice were sacrificed 24 h after APAP injection. Images are representative of at least five independent experiments. Bar, 0.5 mm.

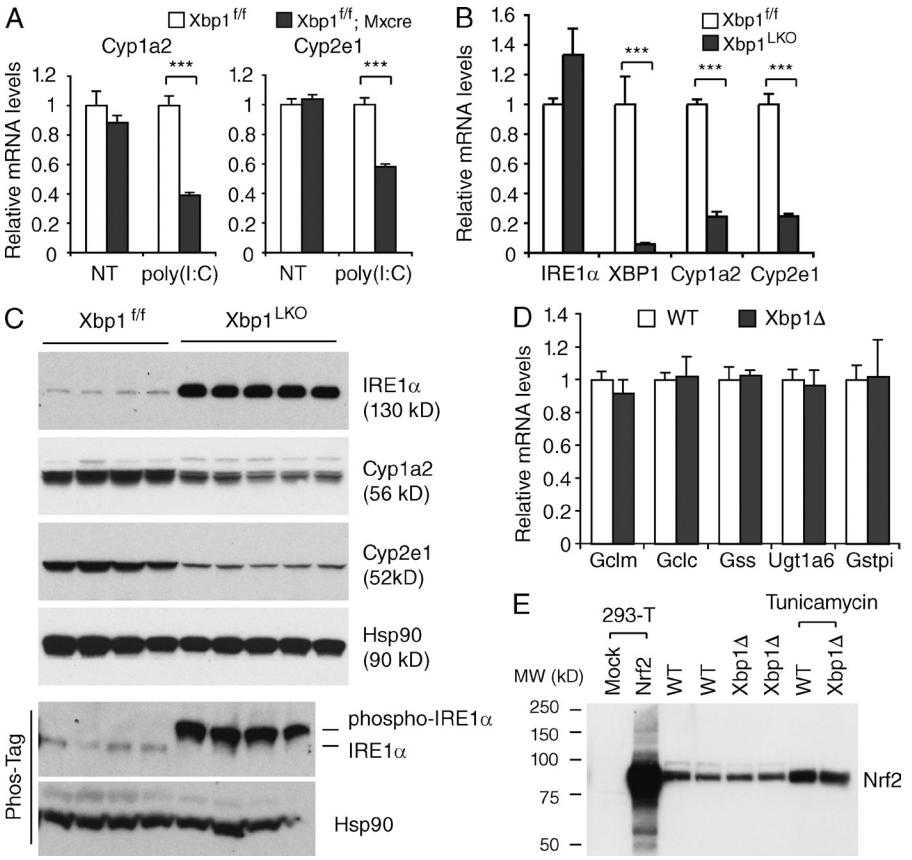

Figure 3. Decreased expression of Cyp1a2 and Cyp2e1 mRNAs in XBP1-deficient liver accompanied by constitutive activation of IRE1α. (A) Total RNAs were isolated from the liver of Xbp1$^{f/f}$;Mx1-cre and the control Xbp1$^{f/f}$ mice untreated (NT) or injected with poly (I:C) 3 wk before sacrifice. Cyp1a2 and Cyp2e1 mRNA levels were measured by qRT-PCR. $n = 3$–4 mice per group. (B) qRT-PCR analysis of the liver of Xbp1^{LKO} and control Xbp1$^{f/f}$ mice. $n = 3$–5 mice per group. ***, $P < 0.001$. (C) Liver lysates were isolated from Xbp1$^{f/f}$ and Xbp1^{LKO} mice and subjected to Western blot analysis. Phos-Tag gel electrophoresis was performed to better separate phosphorylated IRE1α from the unphosphorylated form. (D) qRT-PCR analysis of genes involved in antioxidant responses and drug metabolism regulated by Nrf2. $n = 4$ mice per group. (E) Nrf2 protein levels were determined by Western blot of liver nuclear extracts. Lysates from 293T cells transfected with Nrf2 plasmid or mock transfected served as control. Data are representative of at least three independent experiments.

detoxification system of the liver (Fig. 4 A). Xbp1^{LKO} mice exhibited slightly faster recovery of GSH levels than WT mice, suggesting that the burden of toxic APAP metabolites was lower in the former (Fig. 4 A). In contrast, APAP-conjugated protein adducts were not substantially reduced in the XBP1-deficient liver, suggesting that the residual level of these P450 enzymes is sufficient to generate APAP adducts (Fig. 4, B and C).

JNK is activated by APAP-induced oxidative stress and plays a crucial role in the hepatotoxicity (Gunawan et al., 2006; Henderson et al., 2007; Kaplowitz et al., 2008; Nakagawa et al., 2008). To determine the effect of XBP1 ablation on JNK activation, we measured the level of JNK phosphorylation in liver tissues by Western blotting after APAP treatment. In WT mice, JNK phosphorylation was strongly induced for 6 h after APAP treatment, and then declined at the 24-h time point to low, but detectable levels, reflecting the prolonged oxidative stress (Fig. 4, B and C). Xbp1^{LKO} mice also exhibited marked induction of JNK phosphorylation at early time points (Fig. 4 B), consistent with GSH depletion and APAP adduct formation. Notably, JNK phosphorylation was decreased to baseline levels at the 24-h time point in Xbp1^{LKO} mice, in contrast to the markedly higher levels in WT mice (Fig. 4 C), suggesting that the lack of prolonged JNK activation might contribute to the protection of XBP1-deficient mice from APAP-induced hepatotoxicity. Given that Cyp2e1 generates reactive oxygen species by metabolizing a variety of substrates (Cederbaum et al., 2009), it is conceivable that the reduction of Cyp2e1 in XBP1-deficient liver might ameliorate oxidative stress and JNK activation.

Inverse correlation between IRE1α activation and mRNA levels of Cyp1a2 and Cyp2e1

Because XBP1 is a transcriptional activator, we first sought to determine if XBP1 directly induced the transcription of Cyp1a2 and Cyp2e1. Contrary to our prediction, adenoviral overexpression of XBP1s failed to induce these P450 enzyme mRNAs in primary hepatocytes (Fig. 5 A). Furthermore, tunicamycin injection decreased hepatic Cyp1a2 and Cyp2e1 mRNA levels, despite a strong induction of XBP1s and its target genes, BiP and ERdj4, arguing against a direct role of XBP1 in regulating these genes (Fig. 5, B and C).

Previously, we reported that the ablation of XBP1 led to feedback activation of its upstream enzyme IRE1α in the liver (Lee et al., 2008). IRE1α hyperactivation in XBP1-deficient liver appeared to be an ER stress–independent event, given that ER morphology was normal and activation of other UPR branches was unaltered. Interestingly, recent studies have demonstrated that IRE1α can induce the degradation of certain mRNAs, a process known as regulated IRE1-dependent decay (RIDD; Han et al., 2009; Hollien et al., 2009; Oikawa et al., 2010). In contrast to the efficient relegation of XBP1 mRNA after cleavage by IRE1α, in RIDD, mRNA substrates appear to be degraded after the cleavage, presumably by cellular ribonucleases (Lipson et al., 2008; Han et al., 2009; Hollien et al., 2009; Oikawa et al., 2010; Lee et al., 2011). These observations

prompted us to test if the constitutively active IRE1α induced the degradation of Cyp1a2 and Cyp2e1 mRNAs in XBP1-deficient liver.

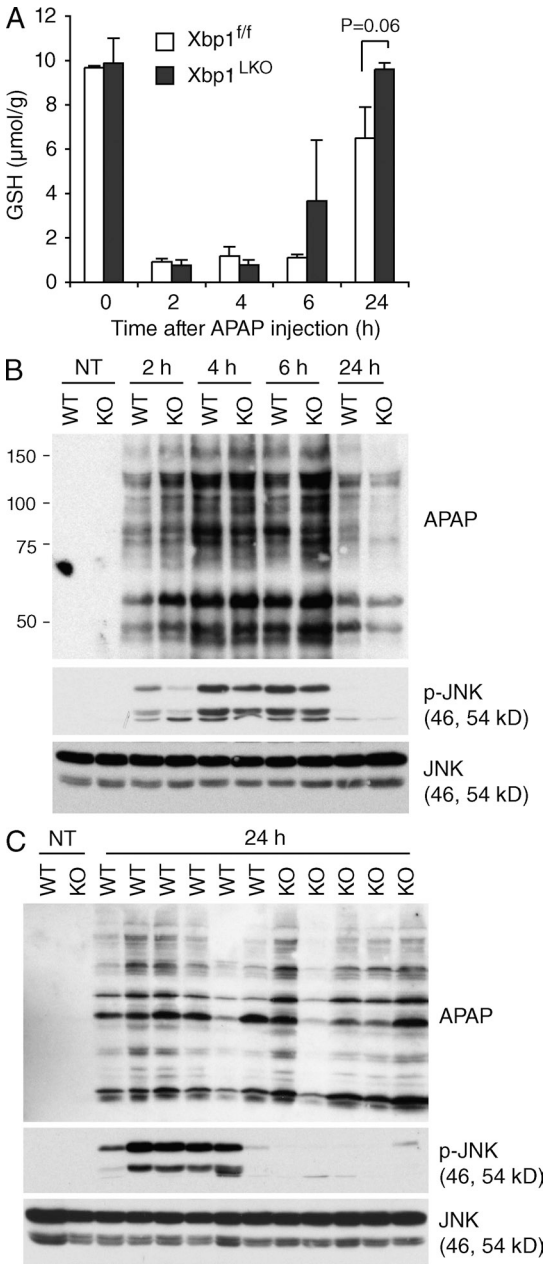

Figure 4. Effects of APAP on hepatic GSH levels and the formation of APAP-protein adducts in WT and Xbp1^{LKO} mice. (A) Hepatic GSH levels were measured at various time points after 500 mg/kg APAP injection. n = 3–6 mice per group. Values represent means ± SEM. (B) Mice were sacrificed at indicated time points after APAP injection. Liver lysates of WT and Xbp1^{LKO} mice (KO) were prepared and pooled for Western blot analysis using anti-APAP, anti-phospho-JNK, and total JNK antibodies. (C) Liver lysates from individual mice treated with APAP for 24 h or left untreated (NT) were subjected to Western blot analysis. Note that the blot was exposed to x-ray film longer than in B to increase the sensitivity.

Western blot analysis of liver lysates revealed that IRE1α protein was induced and constitutively phosphorylated in the liver of Xbp1^{LKO} mice, consistent with what has been observed in Xbp1Δ mice (Fig. 3 C). Phos-Tag SDS-PAGE analysis demonstrated that IRE1α phosphorylation was dramatically induced in XBP1-deficient liver, indicating the constitutive activation of IRE1α in the mutant mice (Fig. 3 C). To investigate if the hyperactivated IRE1α down-regulated Cyp1a2 and Cyp2e1 in XBP1-deficient liver, we suppressed IRE1α expression in the liver of Xbp1^{LKO} mice using siRNA. Intravenous injection of lipidoid-formulated siRNA targeting IRE1α efficiently reduced IRE1α mRNA and protein levels in XBP1-deficient liver (Fig. 6). Notably, IRE1α siRNA markedly induced hepatic Cyp1a2 and Cyp2e1 at both mRNA and protein levels in the liver of Xbp1^{LKO} mice (Fig. 6). These data indicate that constitutively active IRE1α decreased Cyp1a2 and Cyp2e1 mRNAs in XBP1-deficient liver, presumably through RIDD.

ER stress induces IRE1α mediated degradation of Cyp1a2 and Cyp2e1 mRNAs

Decreased expression of Cyp1a2 and Cyp2e1 mRNAs in tunicamycin-injected mice suggests that ER stress might also activate RIDD, leading to the degradation of these mRNAs (Fig. 5 C). To further investigate the link between the ER stress response and APAP metabolism, we characterized the phenotype of IRE1α-deficient mice, which were generated by crossing Ern1 flox mice (Iwawaki et al., 2010) with Mx1-cre transgenic mice. IRE1α deletion in the liver was achieved by poly(I:C) injection, as done previously to generate Xbp1Δ mice (Lee et al., 2008). Cre-mediated deletion of exons 20 and 21 of Ern1 caused an in-frame deletion of 64 aa (aa 844–907) in the ribonuclease domain of IRE1α, which completely abolished its ribonuclease activity, thus abrogating XBP1 mRNA splicing in the mutant mice (Fig. 7, A and B; Iwawaki et al., 2010). Consistent with what we observed in Xbp1Δ mice (Lee et al., 2008), ablation of IRE1α abolished the induction of XBP1-dependent UPR genes such as ERdj4 and Sec61α in the liver of tunicamycin-injected mice (Fig. 7 C). Expression of CHOP, which is known to be regulated primarily by the PERK pathway, was not significantly altered in IRE1α-deficient liver at the basal state or after tunicamycin treatment (Fig. 7 C). Notably, however, hepatic Cyp1a2 and Cyp2e1 mRNA levels were comparable between WT and Ern1Δ mice, in contrast to the significant reduction of these mRNAs in XBP1-deficient mouse liver. Further, Cyp1a2 and Cyp2e1 mRNAs were markedly decreased by tunicamycin treatment in WT but not IRE1α-deficient mice, indicating that these mRNAs were down-regulated by IRE1α in response to ER stress (Fig. 7 C). Consistent with the normal expression of Cyp1a2 and Cyp2e1 mRNAs in Ern1Δ mice, APAP-induced hepatotoxicity was comparable between WT and IRE1α-deficient mice, as assessed by serum ALT levels and histological analysis (Fig. 7, D and E). However, Ern1Δ mice were not more sensitive to APAP-induced hepatotoxicity than WT mice when challenged with a reduced dose of APAP,

suggesting that basal IRE1α activity is not sufficient to confer a protective effect. In conclusion, removal of IRE1α stabilized Cyp1a2 and Cyp2e1 mRNAs and also removed protection from APAP-induced hepatotoxicity conferred by XBP1 deficiency.

Cleavage of Cyp1a2 and Cyp2e1 mRNAs by IRE1α

To ascertain that Cyp1a2 and Cyp2e1 mRNAs are indeed degraded after cleavage by IRE1α, we first tested if IRE1α activation by transient overexpression suppressed the production of these mRNAs. We co-transfected HEK293T cells with Cyp1a2 and Cyp2e1 plasmids, along with WT or an inactive mutant IRE1α. Expression of Cyp1a2 and Cyp2e1 mRNAs was markedly suppressed by the co-transfected WT, but not mutant IRE1α (Fig. 8 A). Similarly, co-transfected IRE1α reduced expression of Bloc1s1 mRNA, which has been identified as an IRE1α substrate for degradation in previous studies (Han et al., 2009; Hollien et al., 2009).

To directly demonstrate the cleavage of mRNAs by IRE1α, we next generated Cyp1a2 and Cyp2e1 mRNAs by in vitro transcription and incubated them with recombinant IRE1α protein. In a control experiment, IRE1α efficiently cleaved XBP1 mRNA, generating two fragments with the expected sizes, indicating that the cleavage occurred at the correct sites (Fig. 8 B). Notably, Cyp1a2 and Cyp2e1 mRNAs were also cleaved by IRE1α to smaller fragments (Fig. 8 B). As a negative control, β-actin mRNA was not cleaved by IRE1α. To determine if IRE1α could cleave endogenously produced Cyp1a2 and Cyp2e1 mRNAs, we incubated recombinant IRE1α protein with total RNA isolated form mouse liver (Fig. 8 C). Northern blot analysis demonstrated that IRE1α

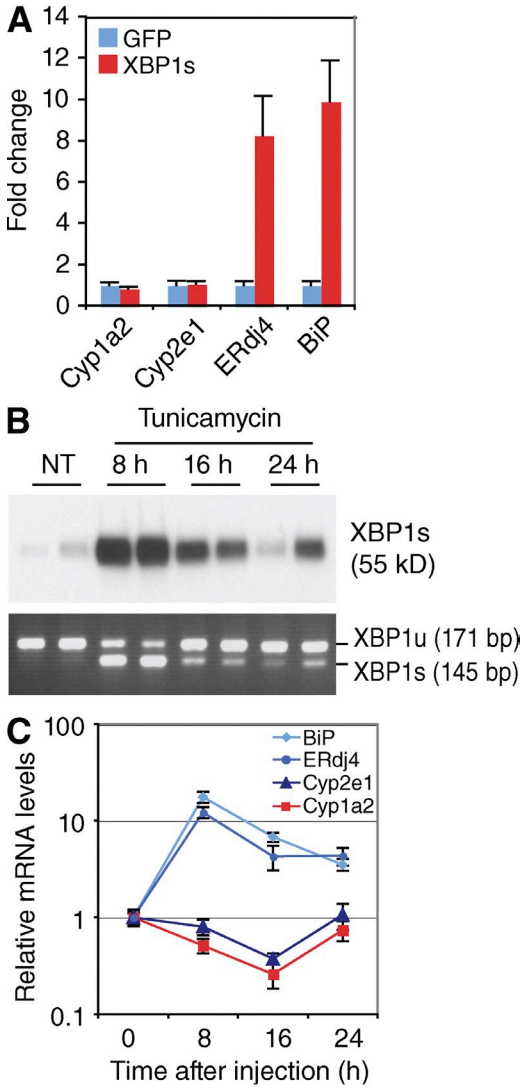

Figure 5. Suppression of Cyp1a2 and Cyp2e1 mRNA expression by ER stress. (A) Mouse primary hepatocytes were infected with adenovirus expressing GFP or XBP1s. RNAs were isolated 24 h after viral infection for RT-PCR analysis. Data are mean ± SEM from quadruplicate samples. (B) Mice were i.p. injected with tunicamycin (1.5 mg/kg). IRE1α-mediated XBP1 mRNA splicing and the level of XBP1s protein were measured by RT-PCR and Western blot, respectively. Data shown are from two independently treated mice. Each lane represents an individual mouse. (C) mRNA levels of indicated genes in the liver of tunicamycin-injected mice measured by qRT-PCR. *n* = 2 mice per group.

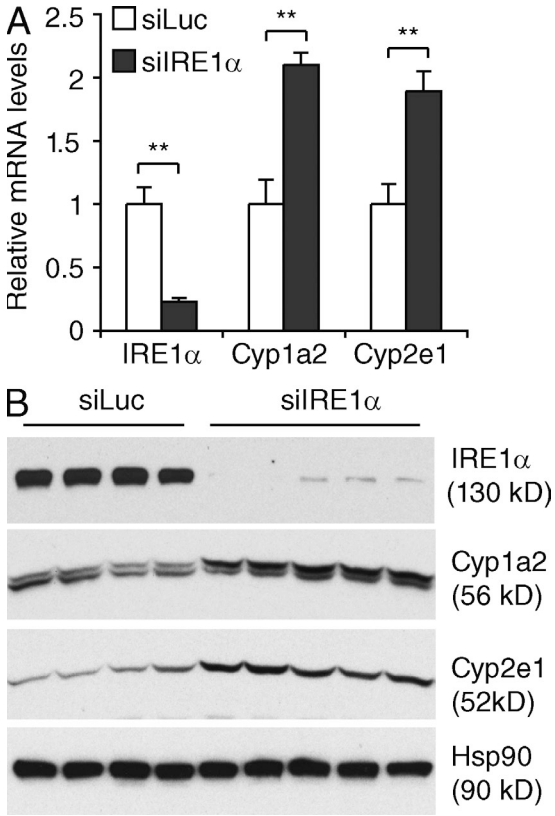

Figure 6. Induction of Cyp1a2 and Cyp2e1 mRNAs by siRNA targeting IRE1α in XBP1-deficient liver. (A) $Xbp1^{LKO}$ mice were injected with lipidoid-formulated siRNAs targeting IRE1α or luciferase. 8 d later, mice were sacrificed to isolate RNA and protein from the liver for qRT-PCR and Western blot analysis (B). *n* = 3–5 mice per group. **, P < 0.01.

cleaved Cyp1a2 and Cyp2e1 mRNAs at specific sites, yielding smaller fragments that were largely comparable to the cleavage products of in vitro–transcribed mRNAs (Fig. 8, B and C). XBP1 mRNA was also efficiently cleaved by IRE1α, generating a smaller fragment that was detected by a probe hybridizing to the 3′ end of the mRNA. In contrast, β-actin and Cyp2c29 mRNAs, which were normally expressed in Xbp1-deficient liver were unaffected by recombinant IRE1α protein (Fig. 8 C), indicating the specific cleavage of Cyp1a2 and Cyp2e1 mRNAs by IRE1α.

To determine IRE1α cleavage sites in Cyp1a2 and Cyp2e1 mRNAs, we performed 5′ rapid amplification of cDNA ends (RACE) PCR on in vitro–transcribed mRNAs after IRE1α cleavage. This procedure identified one cleavage site in Cyp1a2 and four sites in Cyp2e1 mRNAs (Fig. 8 D). DNA sequencing of PCR products revealed that IRE1α cleaves at G–C junctions within 5′-CUGCAG-3′ consensus sequences, which are conserved in XBP1 and in other RIDD substrate mRNAs (Oikawa et al., 2010). Although secondary structure prediction of individual IRE1α cleavage sites yielded dissimilar hairpin structures, sequence alignment of the cleavage sites generated a consensus secondary structure that was congruent with the XBP1 hairpin, suggesting that IRE1α recognizes a common secondary structure in target mRNAs (Fig. 8 D). Mutation of two G residues at −1 and +3 positions in the consensus sequence abolished the cleavage of Cyp1a2 and Cyp2e1 mRNAs by IRE1α (Fig. 8, E–G), indicating that these residues are essential for IRE1α cleavage. Collectively, these data demonstrate that hyperactivated IRE1α specifically cleaves Cyp1a2 and Cyp2e1 mRNAs in XBP1-deficient liver, leading to further degradation by cellular ribonucleases.

APAP does not activate UPR in the liver

Recent studies demonstrated the association of ER stress response with a variety of liver diseases (Ji, 2008). APAP is known to activate ER stress response (Lorz et al., 2004; Nagy et al., 2007), an observation that invites the speculation that feedback activation of IRE1α by APAP may suppress the production of NAPQI driven by Cyp1a2 and Cyp2e1. However, we did not observe the activation of IRE1α or other UPR branches such as PERK and ATF6α in the liver of APAP-treated mice, arguing against a role of APAP in IRE1α activation (Fig. 9). Physiological and pathological conditions that activate IRE1α, leading to the degradation of Cyp1a2 and Cyp2e1 mRNAs, remained to be explored.

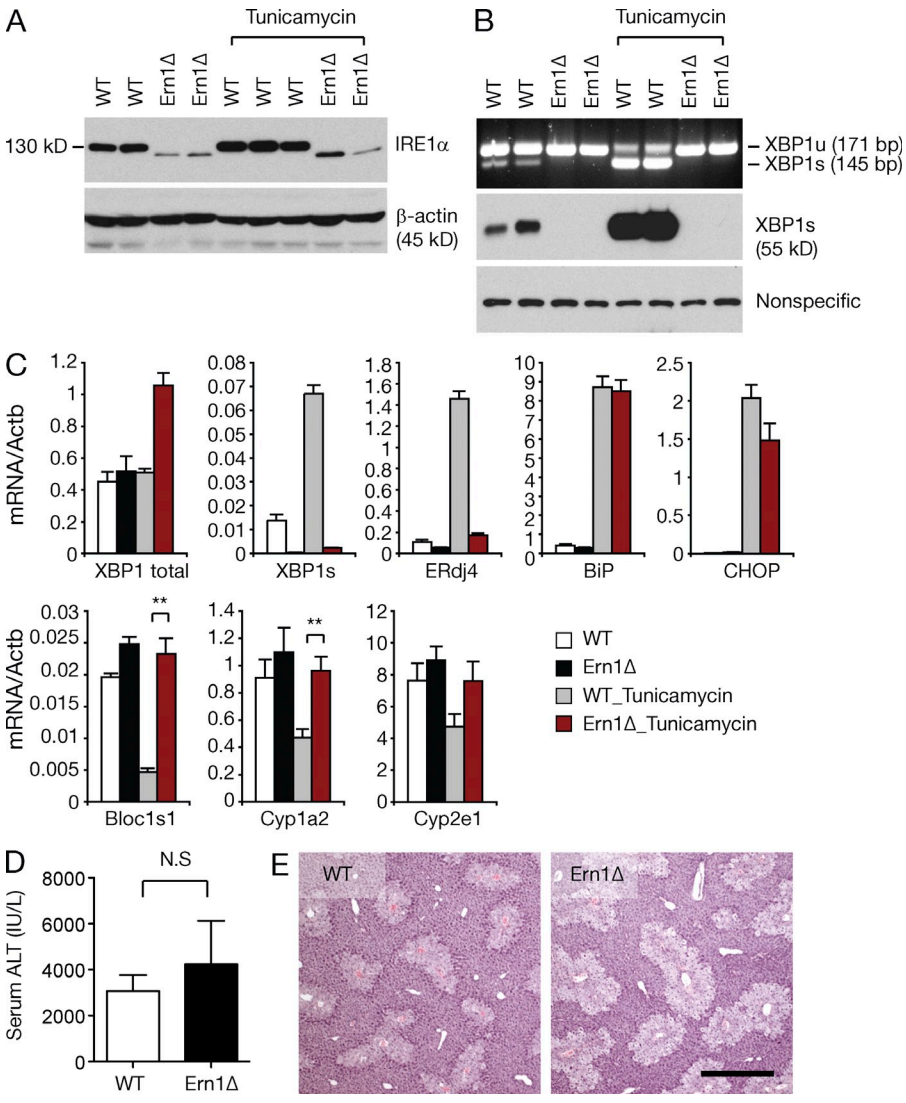

Figure 7. Effects of tunicamycin on gene expression in IRE1α–deficient liver. (A) WT or Ern1Δ mice were untreated or injected i.p. with tunicamycin (1.5 mg/kg) 6 h before sacrifice. Liver lysates were subjected to Western blot analysis of IRE1α. Ern1Δ mice expressed a mutant IRE1α lacking 64 amino acids in the ribonuclease domain. (B) RT-PCR was performed to measure XBP1 mRNA splicing. XBP1s protein level was determined by Western blot using liver nuclear extracts. Data are representative of more than two independent experiments. (C) WT and Ern1Δ mice were injected with tunicamycin (1.5 mg/kg) and hepatic gene expression examined before and 6 h after tunicamycin injection. $n = 4–6$ mice per group. $^{**}P < 0.01$. (D) Mice were i.p. injected with 300 mg/kg APAP, and then bled 24 h later for ALT assays. $n = 6–8$ mice per group. (E) H&E staining of liver sections. Images are representative of at least five independent experiments. Mice were sacrificed 24 h after APAP injection. Bar, 0.5 mm.

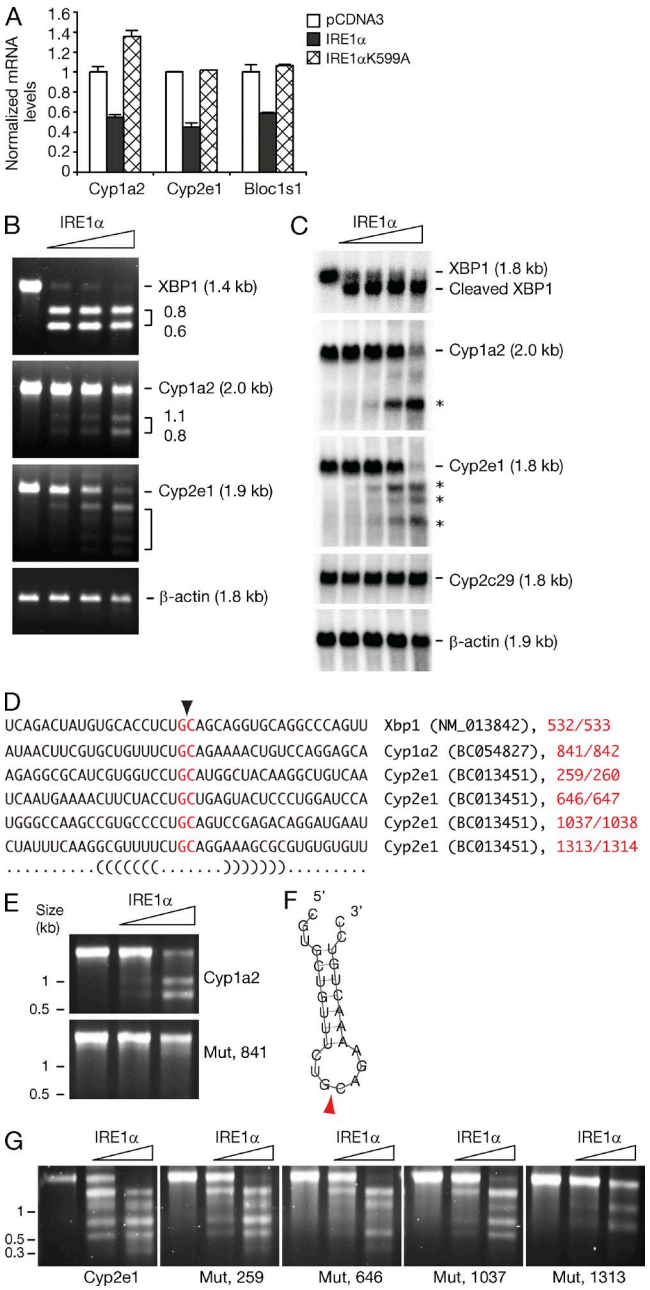

Figure 8. XBP1 deficiency induces feedback activation of IRE1α, resulting in IRE1α–mediated mRNA degradation of select p450 genes. (A) 293T cells were co-transfected with CMV SPORT6-EGFP, CMV SPORT6-Cyp1a2, CMV SPORT6-Cyp2e1, and CMV SPORT6-Bloc1s1 together with empty, WT, or K599A mutant IRE1α plasmids. Cells were harvested 24 h after transfection to measure the expression levels of the transfected genes. mRNA levels were measured by qRT-PCR and normalized to the co-transfected EGFP. Independent experiments were repeated at least three times and the representative result is shown. (B) Recombinant IRE1α was incubated with RNA substrates generated by in vitro transcription using SP6 RNA polymerase. Reaction mixtures were run on denaturing agarose gels, which were then stained with ethidium bromide. Data are representative of two independent experiments. (C) In vitro cleavage assay was performed using liver RNA as substrate. Northern blot was performed to reveal mRNA cleavage. β-Actin and Cyp2c29 mRNAs are shown as a control. Asterisks represent IRE1α-cleaved mRNA species. (D) Nucleotide sequences around IRE1α cleavage sites in Cyp1a2 and Cyp2e1 mRNAs. IRE1α cleaves G/C junctions shown in red. Matching brackets represent base pairs of the consensus secondary structure. (E) In vitro IRE1α cleavage assay of WT and mutant Cyp1a2 mRNA. (F) Predicted secondary structure of IRE1α cleavage site in Cyp1a2 mRNA. Arrowhead indicates the cleavage site. Two G residues (italicized) were changed to T to generate the mutant construct used in E. (G) In vitro IRE1α cleavage assay of WT and mutant Cyp2e1 mRNAs. Data are representative of two independent experiments.

DISCUSSION

RIDD was first described in *Drosophila melanogaster* cells, where IRE1 was observed to induce the degradation of mRNAs encoding proteins that transit through the ER (Hollien and Weissman, 2006). Subsequent studies in mammalian cells reported that IRE1α suppressed the expression not only of secretory pathway cargo proteins, but also ER-resident proteins that handle the folding and trafficking of cargo proteins (Han et al., 2009). These observations raised the possibility that RIDD might act as a novel mechanism to alleviate ER stress by limiting the entry of cargo proteins into the ER. It was also possible that RIDD could exert opposing effects on cell fate, such that it might maintain homeostasis by acutely relieving ER stress, but promote apoptosis under conditions of prolonged, high level ER stress (Han et al., 2009; Hollien et al., 2009). However, the in vivo functions of RIDD in physiological or pathological situations remained to be explored. Here, we demonstrate that IRE1α hyperactivation in hepatocytes in vivo led to RIDD that resulted in protection from the stress of a hepatotoxic APAP metabolite. Our study reveals that the IRE1α–XBP1 UPR signaling pathway plays a key role in hepatic drug metabolism, at least in part by regulating the stability of certain p450 mRNAs by RIDD.

Important RIDD substrates in the liver include, but may not be limited to, mRNAs encoding the key p450 drug-metabolizing enzymes Cyp1a2 and Cyp2e1. Reduction of Cyp1a2 and Cyp2e1 mRNAs correlated with the protection of XBP1-deficient mice from APAP-induced hepatotoxicity, although it remains to be determined if the reduction of these mRNAs is sufficient for protection. Acute GSH depletion and APAP-protein adduct formation were not significantly altered in XBP1-deficient liver upon APAP treatment, raising the possibility that Cyp1a2- and Cyp2e1-independent mechanisms might contribute to the protection of XBP1-deficient mice from APAP-induced hepatotoxicity. There may well be additional RIDD substrates involved in APAP metabolism required to confer protection from APAP-induced hepatotoxicity.

JNK is activated by oxidative stress, and plays a central role in APAP-induced hepatotoxicity (Gunawan et al., 2006; Henderson et al., 2007; Kaplowitz et al., 2008; Nakagawa et al., 2008). IRE1α activates JNK under ER stress conditions (Urano et al., 2000). However, JNK was not induced in XBP1-deficient liver, despite the presence of hyperactivated IRE1α, indicating that IRE1α is not sufficient to activate JNK.

Indeed, XBP1-deficient liver instead exhibited reduced JNK activation upon APAP treatment, which might contribute to the observed protection from APAP-induced hepatotoxicity.

In normal mouse liver, IRE1α is present mostly in an inactive form, as indicated by minimal phosphorylation of IRE1α and low levels of XBP1 mRNA splicing. Ablation of IRE1α did not significantly decrease Cyp1a2 and Cyp2e1 mRNA levels, suggesting that the basal IRE1α activity present in normal mouse liver is not sufficient to cause a significant reduction of its substrate mRNAs. Pathophysiological conditions that activate IRE1α to instigate RIDD in genetically intact animals remain to be identified. Interestingly, it has previously been shown that high-fat and high-cholesterol diets promote the degradation of MTP mRNA in the intestine by gut-restricted IRE1β protein, suppressing chylomicron production (Iqbal et al., 2008). IRE1α did not cleave MTP mRNA, indicating the divergent substrate specificities of IRE1α and IRE1β (Iqbal et al., 2008). Various insults to hepatocytes, such as fat accumulation, viral infection, inflammation, hyperhomocysteinemia, and oxidative stress, have been implicated in the ER stress response in the liver (Ji, 2008), and it would be interesting to see if RIDD is instigated under these conditions.

Hyperactivation of IRE1α either through elimination of its substrate XBP1 or through pharmacologically induced ER stress can instigate RIDD. The fact that XBP1 deficiency causes hyperactivation of IRE1α which can induce the degradation of certain mRNAs raises an interesting question. Ablation of XBP1 causes multiple abnormalities in many organ systems in mice, which include the deficiency of professional secretory cells (Reimold et al., 2001; Lee et al., 2005; Kaser et al., 2008; Huh et al., 2010), defective insulin secretion from β cells (Lee et al., 2011), decreased lipogenesis in the liver (Lee et al., 2008), and impaired cytokine production from macrophages (Martinon et al., 2010). What are the relative contributions of these two functions of IRE1α, one of them XBP1-independent (RIDD) and the other dependent on XBP1-driven gene regulation, to the phenotypes of XBP1-deficient mice? As we have done here, it will be critical to compare the phenotypes of XBP1 and IRE1α single and XBP1–IRE1α double-deficient mice in each organ to answer this question. Such studies are currently underway and should establish the contribution of indirect IRE1α hyperactivation (RIDD) induced by XBP1 deficiency versus a direct effect of XBP1 deficiency in vivo. We would predict, and our early studies support, that this balance will be different in different organ systems (Lee et al., 2008).

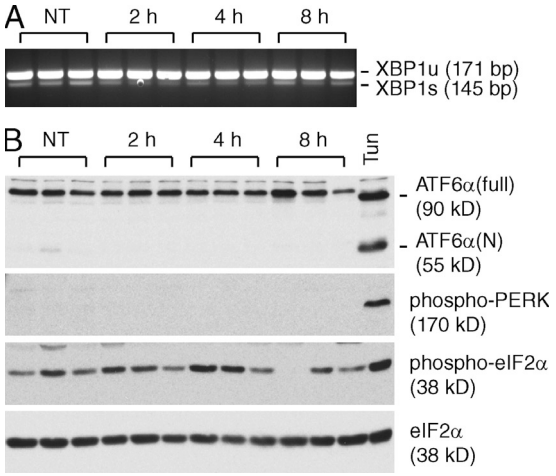

Figure 9. APAP does not induce the UPR in liver. (A) Mice were injected i.p. with 500 mg/kg APAP after a 16-h fast, and then sacrificed at indicated time points. XBP1 mRNA splicing in the liver was measured by RT-PCR as a marker of IRE1α activity. (B) Western blot analysis of whole-liver lysates. Liver lysate of a tunicamycin-treated mouse was included as a positive control. Each lane represents an individual mouse.

It is notable that there are both similarities and disparities between the phenotypes of XBP1 and IRE1α knock out mice. At the molecular level, Ern1 deletion abolishes the expression of both IRE1α and XBP1s. In contrast, Xbp1 deletion abolishes the expression of XBP1u and XBP1s, but activates IRE1α in certain organs and cell types, such as liver, intestinal epithelium, β cells, and macrophages; however, XBP1 does not activate IRE1α in neurons. Germ line deletion of *Ern1* or *Xbp1* caused embryonic lethality in mice because of impaired liver development (Reimold et al., 2000; Zhang et al., 2005). Interestingly, the embryonic lethal phenotypes of these mice were reversed by expression of IRE1α in the placenta or XBP1 in the liver (Iwawaki et al., 2009; Lee et al., 2005), indicating differential requirements for IRE1α and XBP1 in the development of these organs. XBP1- and IRE1α-deficient mice display abnormalities in secretory cells and organs, but the latter appear to have milder phenotypes (Reimold et al., 2001; Lee et al., 2005; Iwawaki et al., 2010). One exception to this, however, is in the B cell lineage, where IRE1α-deficient chimeras display a halt in B cell differentiation at an early stage of B cell development (Zhang et al., 2005) in contrast to XBP1 lymphoid chimeras or B cell–specific $Xbp1^{f/f}$;$CD19^{+/cre}$ mice where B cell development proceeds normally until the terminal stage of B cell differentiation to plasma cells (Reimold et al., 2000; Todd et al., 2009). It remains to be determined if this difference in timing and severity of phenotype is caused by a contribution by RIDD or can be explained by different experimental settings, such as mouse genetic background.

Although basal IRE1α activity is low in normal mouse liver, it is sufficient to drive the production of measurable amounts of XBP1s protein. Remarkably, ablation of XBP1 induces a striking activation of its upstream endoribonuclease IRE1α in a feedback loop whose components are unknown. It is notable that ablation of XBP1 activated IRE1α, but not PERK or ATF6, in the liver, although a pharmacologic ER stress inducer, tunicamycin, simultaneously activated all three UPR branches (Lee et al., 2008), suggesting that the signal activating IRE1α might be distinct from those for other UPR branches. Identifying the molecular constituents of this regulatory circuit is an important goal of future studies.

MATERIALS AND METHODS

Mice. Generation of Xbp1Δ mice ($Xbp1^{f/f}$;Mx1-cre mice injected with poly [I:C]) has been previously described (Lee et al., 2008). IRE1α-deficient Ern1Δ mice were generated by breeding $Ern1^{flox}$ mice (Iwawaki et al., 2009) with Mx1-cre mice, and then i.p. injecting 250 µg of poly(I:C) twice into $Ern1^{f/f}$;Mx1-cre mice. B6.Cg-Tg(Alb-cre)21Mgn/J mice that contained an albumin promoter-driven Cre recombinase transgene were obtained from The Jackson Laboratory and crossed with $Xbp1^{flox}$ mice to generate $Xbp1^{LKO}$ mice. Animal studies and experiments were approved and performed according to the guidelines of the Animal Care and Use Committee of Harvard University.

APAP-induced hepatotoxicity. APAP (Sigma-Aldrich) was dissolved in 1,2-propanediol-saline (50:50) solution at 50 mg/ml. After a 16-h fast, mice were injected i.p. with freshly prepared APAP solution at 500 mg/kg of body weight, unless otherwise indicated. Blood was drawn from tail vein to measure ALT activity using a commercial reagent (Bio-Quant). Plasma samples were serially diluted threefold in PBS to obtain the ALT level within the detection range of the reagent. Liver tissue samples were fixed in 10% neutral buffered formalin, embedded in paraffin, cut into 5-µm-thick sections, and stained with hematoxylin and eosin. Hepatic GSH content was measured using a Total *GSH* Quantification kit (Dojindo Molecular Technologies).

In vivo siRNA delivery. Lipidoid-siRNA formulations using C12-200 were prepared as described previously (Love et al., 2010). Lipidoid-formulated siRNAs were diluted to 0.1 mg/ml in PBS and administered to mice via tail vein at a dose of 0.5 mg/kg body weight.

RNA isolation and qRT-PCR. Total RNA was isolated from liver tissue and transfected 293T cells using Qiazol lysis reagent (QIAGEN). SYBR green-based qRT-PCR was performed using the Mx3005P system (Stratagene), with the complementary DNA (cDNA) made using High Capacity cDNA Reverse Transcription kit (Applied Biosystems).

Transfection assays. HEK293T cells were grown in DME supplemented with 10% fetal bovine serum. 150,000 cells were plated in a 12-well plate and transfected with total 1 µg DNA (450 ng pED-IRE1α, 10 ng pCMV-SPORT6-Angplt3, 10 ng pCMV-SPORT6-Bloc1s1, 10 ng pCMV-SPORT6-EGFP, and 520 ng pCMV-SPORT6) using Lipofectamine 2000 (Invitrogen). Cells were harvested 24 h after transfection to extract RNA, which were treated with DNase I (Invitrogen) and subjected to qRT-PCR analysis. Transgenic mRNA levels were normalized to the co-transfected EGFP level.

Western blot. Liver lysates were prepared by homogenization in RIPA buffer (50 mM Tris–Cl pH 8.0, 150 mM NaCl, 1% NP-40, 0.5% deoxycholate, 0.1% SDS, 50 mM NaF) supplemented with protease inhibitor tablet (Roche). Liver nuclear extracts were prepared as described previously (Lee et al., 2008). Phos-tag acrylamide reagent (NARD Institute, Ltd.) and $MnCl_2$ were added to the gel to final concentrations of 10 and 20 µM, respectively, for Phos-Tag gel electrophoresis. Rabbit polyclonal antibody raised against mouse XBP1s, ATF6α, and Nrf2 (McMahon et al., 2003) were used to detect nuclear XBP1s, ATF6α(N), and Nrf2 proteins by Western blot. Anti-APAP (Matthews et al., 1996), anti-Cyp1a2 (Detroit R&D), anti-Cyp2e1 (Detroit R&D), anti-IRE1α (Cell Signaling Technology), anti–phospho-PERK (Cell Signaling Technology), anti-JNK (Cell Signaling Technology), and anti–phospho-JNK (Cell Signaling Technology) antibodies were used to detect specific proteins in whole-liver lysates by Western blot.

Adenoviral overexpression of XBP1s in primary hepatocytes. Recombinant adenoviruses expressing GFP or mouse XBP1s and infection of mouse primary hepatocytes were described previously (Lee et al., 2008). Primary hepatocytes were infected with recombinant adenoviruses at 10 PFU per cell and harvested 24 h later to isolate RNAs for gene expression analysis.

In vitro IRE1α-mediated mRNA cleavage assays. In vitro mRNA cleavage assays were performed as described previously (Lee et al., 2011). In brief, twofold serially diluted recombinant protein containing the cytoplasmic domain of human IRE1α (28, 14, 7, and 3.5 ng) was incubated with 1 µg of RNA generated by in vitro transcription using SP6 or T7 polymerase (Invitrogen) and specific MGC cDNA clones in pCMV-SPORT6 vector (Open Biosystems), or 3 µg of total liver RNA for 30 min at 37°C. IRE1α-mediated cleavage of in vitro–transcribed RNA was revealed by ethidium bromide staining of the agarose gel after electrophoresis. Liver RNA treated with IRE1α was resolved on denaturing agarose gels and subjected to Northern blot analysis. Radiolabeled probes were prepared using Rediprime II random prime labeling system (GE Healthcare). Templates for radiolabeled probes were generated by PCR amplification of the fragments of Cyp1a2 (+1 to +1093, BC064827), Cyp2c29 (+9 to +412, BC019908), and Cyp2e1 (+1 to +512, BC013451) cDNAs.

Identification of IRE1α cleavage sites in Cyp1a2 and Cyp2e1 mRNAs. Cyp1a2 and Cyp2e1 mRNAs produced by in vitro transcription were incubated with recombinant IRE1α. IRE1α-cleaved RNAs were treated with T4 polynucleotide kinase, and then ligated with 5′-RACE adapter (5′-GCUGAUGGCGAUGAAUGAACACUGCGUUUGCUGGCUUUGAUGAAA-3′; Invitrogen) using T4 RNA ligase (New England BioLabs). After a purification step using RNeasy MinElute Cleanup kit (QIAGEN), ligated RNAs were subjected to cDNA synthesis followed by PCR amplification using RACEouter primer (5′-GCTGATGGCGATGAATGAACACTG-3′) and various reverse primers that anneal to Cyp1a2 and Cyp2e1 mRNAs with 300–400-bps intervals. PCR products were subjected to DNA sequencing.

Online supplemental material. Table S1 shows the expression of genes related to drug metabolism in XBP1-deficient liver. Online supplemental material is available at http://www.jem.org/cgi/content/full/jem.20111298/DC1.

We thank Dr. Dean Roberts for anti-APAP antibody, Dr. Michael McMahon for anti-Nrf2 antibody, Dorothy Hu for histological analysis, Kirsten Sigrist for animal maintenance, and Drs. Fabio Martinon and Eun-Sook Hwang for critical reading of this manuscript. We also thank Brian Bettencort and Greg Hinkle (design and bioinformatics); Akin Akinc and Alnylam formulations group; and Muthiah Manoharan, Martin Maier, Satya Kumchimanchi, Klaus Charisse, and the rest of the Alnylam chemistry team for siRNA synthesis.

This study was supported by National Institutes of Health grants AI32412 (L.H. Glimcher), DK082448 (L.H. Glimcher), and DK089211 (A.-H. Lee), and a grant from the American Heart Association (A.-H. Lee).

L.H. Glimcher is a Member of the Board of Directors of and holds equity in Bristol Myers Squibb. The other authors have no conflicting financial interests.

Submitted: 24 June 2011
Accepted: 23 December 2011

REFERENCES

Blazka, M.E., J.L. Wilmer, S.D. Holladay, R.E. Wilson, and M.I. Luster. 1995. Role of proinflammatory cytokines in acetaminophen hepatotoxicity. *Toxicol. Appl. Pharmacol.* 133:43–52. http://dx.doi.org/10.1006/taap.1995.1125

Brewer, J.W., and L.M. Hendershot. 2005. Building an antibody factory: a job for the unfolded protein response. *Nat. Immunol.* 6:23–29. http://dx.doi.org/10.1038/ni1149

Calfon, M., H. Zeng, F. Urano, J.H. Till, S.R. Hubbard, H.P. Harding, S.G. Clark, and D. Ron. 2002. IRE1 couples endoplasmic reticulum load to secretory capacity by processing the XBP-1 mRNA. *Nature.* 415:92–96. http://dx.doi.org/10.1038/415092a

Cederbaum, A.I., Y. Lu, and D. Wu. 2009. Role of oxidative stress in alcohol-induced liver injury. *Arch. Toxicol.* 83:519–548. http://dx.doi.org/10.1007/s00204-009-0432-0

Chan, K., and Y.W. Kan. 1999. Nrf2 is essential for protection against acute pulmonary injury in mice. *Proc. Natl. Acad. Sci. USA.* 96:12731–12736. http://dx.doi.org/10.1073/pnas.96.22.12731

Chan, K., X.D. Han, and Y.W. Kan. 2001. An important function of Nrf2 in combating oxidative stress: detoxification of acetaminophen. *Proc. Natl. Acad. Sci. USA.* 98:4611–4616. http://dx.doi.org/10.1073/pnas.081082098

Cohen, S.D., and E.A. Khairallah. 1997. Selective protein arylation and acetaminophen-induced hepatotoxicity. *Drug Metab. Rev.* 29:59–77. http://dx.doi.org/10.3109/03602539709037573

Cox, J.S., C.E. Shamu, and P. Walter. 1993. Transcriptional induction of genes encoding endoplasmic reticulum resident proteins requires a transmembrane protein kinase. *Cell.* 73:1197–1206. http://dx.doi.org/10.1016/0092-8674(93)90648-A

Cribb, A.E., M. Peyrou, S. Muruganandan, and L. Schneider. 2005. The endoplasmic reticulum in xenobiotic toxicity. *Drug Metab. Rev.* 37:405–442. http://dx.doi.org/10.1080/03602530500205135

Gonzalez, F.J. 2007. The 2006 Bernard B. Brodie Award Lecture. Cyp2e1. *Drug Metab. Dispos.* 35:1–8. http://dx.doi.org/10.1124/dmd.106.012492

Gunawan, B.K., Z.X. Liu, D. Han, N. Hanawa, W.A. Gaarde, and N. Kaplowitz. 2006. c-Jun N-terminal kinase plays a major role in murine acetaminophen hepatotoxicity. *Gastroenterology.* 131:165–178. http://dx.doi.org/10.1053/j.gastro.2006.03.045

Han, D., A.G. Lerner, L. Vande Walle, J.P. Upton, W. Xu, A. Hagen, B.J. Backes, S.A. Oakes, and F.R. Papa. 2009. IRE1alpha kinase activation modes control alternate endoribonuclease outputs to determine divergent cell fates. *Cell.* 138:562–575. http://dx.doi.org/10.1016/j.cell.2009.07.017

Hanawa, N., M. Shinohara, B. Saberi, W.A. Gaarde, D. Han, and N. Kaplowitz. 2008. Role of JNK translocation to mitochondria leading to inhibition of mitochondria bioenergetics in acetaminophen-induced liver injury. *J. Biol. Chem.* 283:13565–13577. http://dx.doi.org/10.1074/jbc.M708916200

Henderson, N.C., K.J. Pollock, J. Frew, A.C. Mackinnon, R.A. Flavell, R.J. Davis, T. Sethi, and K.J. Simpson. 2007. Critical role of c-jun (NH2) terminal kinase in paracetamol- induced acute liver failure. *Gut.* 56:982–990. http://dx.doi.org/10.1136/gut.2006.104372

Hollien, J., and J.S. Weissman. 2006. Decay of endoplasmic reticulum-localized mRNAs during the unfolded protein response. *Science.* 313:104–107. http://dx.doi.org/10.1126/science.1129631

Hollien, J., J.H. Lin, H. Li, N. Stevens, P. Walter, and J.S. Weissman. 2009. Regulated Ire1-dependent decay of messenger RNAs in mammalian cells. *J. Cell Biol.* 186:323–331. http://dx.doi.org/10.1083/jcb.200903014

Huh, W.J., E. Esen, J.H. Geahlen, A.J. Bredemeyer, A.H. Lee, G. Shi, S.F. Konieczny, L.H. Glimcher, and J.C. Mills. 2010. XBP1 controls maturation of gastric zymogenic cells by induction of MIST1 and expansion of the rough endoplasmic reticulum. *Gastroenterology.* 139:2038–2049. http://dx.doi.org/10.1053/j.gastro.2010.08.050

Iqbal, J., K. Dai, T. Seimon, R. Jungreis, M. Oyadomari, G. Kuriakose, D. Ron, I. Tabas, and M.M. Hussain. 2008. IRE1beta inhibits chylomicron production by selectively degrading MTP mRNA. *Cell Metab.* 7:445–455. http://dx.doi.org/10.1016/j.cmet.2008.03.005

Iwawaki, T., R. Akai, S. Yamanaka, and K. Kohno. 2009. Function of IRE1 alpha in the placenta is essential for placental development and embryonic viability. *Proc. Natl. Acad. Sci. USA.* 106:16657–16662. http://dx.doi.org/10.1073/pnas.0903775106

Iwawaki, T., R. Akai, and K. Kohno. 2010. IRE1α disruption causes histological abnormality of exocrine tissues, increase of blood glucose level, and decrease of serum immunoglobulin level. *PLoS ONE.* 5:e13052. http://dx.doi.org/10.1371/journal.pone.0013052

James, L.P., P.R. Mayeux, and J.A. Hinson. 2003. Acetaminophen-induced hepatotoxicity. *Drug Metab. Dispos.* 31:1499–1506. http://dx.doi.org/10.1124/dmd.31.12.1499

Ji, C. 2008. Dissection of endoplasmic reticulum stress signaling in alcoholic and non-alcoholic liver injury. *J. Gastroenterol. Hepatol.* 23(Suppl 1):S16–S24. http://dx.doi.org/10.1111/j.1440-1746.2007.05276.x

Kaplowitz, N., M. Shinohara, Z.X. Liu, and D. Han. 2008. How to protect against acetaminophen: don't ask for JUNK. *Gastroenterology.* 135:1047–1051. http://dx.doi.org/10.1053/j.gastro.2008.08.031

Kaser, A., A.H. Lee, A. Franke, J.N. Glickman, S. Zeissig, H. Tilg, E.E. Nieuwenhuis, D.E. Higgins, S. Schreiber, L.H. Glimcher, and R.S. Blumberg. 2008. XBP1 links ER stress to intestinal inflammation and confers genetic risk for human inflammatory bowel disease. *Cell.* 134:743–756. http://dx.doi.org/10.1016/j.cell.2008.07.021

Kaufman, R.J. 1999. Stress signaling from the lumen of the endoplasmic reticulum: coordination of gene transcriptional and translational controls. *Genes Dev.* 13:1211–1233. http://dx.doi.org/10.1101/gad.13.10.1211

Lee, A.H., and L.H. Glimcher. 2009. Intersection of the unfolded protein response and hepatic lipid metabolism. *Cell. Mol. Life Sci.* 66:2835–2850. http://dx.doi.org/10.1007/s00018-009-0049-8

Lee, S.S., J.T. Buters, T. Pineau, P. Fernandez-Salguero, and F.J. Gonzalez. 1996. Role of CYP2E1 in the hepatotoxicity of acetaminophen. *J. Biol. Chem.* 271:12063–12067. http://dx.doi.org/10.1074/jbc.271.20.12063

Lee, K., W. Tirasophon, X. Shen, M. Michalak, R. Prywes, T. Okada, H. Yoshida, K. Mori, and R.J. Kaufman. 2002. IRE1-mediated unconventional mRNA splicing and S2P-mediated ATF6 cleavage merge to regulate XBP1 in signaling the unfolded protein response. *Genes Dev.* 16:452–466. http://dx.doi.org/10.1101/gad.964702

Lee, A.H., G.C. Chu, N.N. Iwakoshi, and L.H. Glimcher. 2005. XBP-1 is required for biogenesis of cellular secretory machinery of exocrine glands. *EMBO J.* 24:4368–4380. http://dx.doi.org/10.1038/sj.emboj.7600903

Lee, A.H., E.F. Scapa, D.E. Cohen, and L.H. Glimcher. 2008. Regulation of hepatic lipogenesis by the transcription factor XBP1. *Science.* 320:1492–1496. http://dx.doi.org/10.1126/science.1158042

Lee, A.H., K. Heidtman, G.S. Hotamisligil, and L.H. Glimcher. 2011. Dual and opposing roles of the unfolded protein response regulated by IRE1alpha and XBP1 in proinsulin processing and insulin secretion. *Proc. Natl. Acad. Sci. USA.* 108:8885–8890. http://dx.doi.org/10.1073/pnas.1105564108

Lipson, K.L., R. Ghosh, and F. Urano. 2008. The role of IRE1alpha in the degradation of insulin mRNA in pancreatic beta-cells. *PLoS ONE.* 3:e1648.

Liu, Z.X., and N. Kaplowitz. 2006. Role of innate immunity in acetaminophen-induced hepatotoxicity. *Expert Opin. Drug Metab. Toxicol.* 2:493–503. http://dx.doi.org/10.1517/17425255.2.4.493

Liu, Z.X., S. Govindarajan, and N. Kaplowitz. 2004. Innate immune system plays a critical role in determining the progression and severity of acetaminophen hepatotoxicity. *Gastroenterology.* 127:1760–1774. http://dx.doi.org/10.1053/j.gastro.2004.08.053

Lorz, C., P. Justo, A. Sanz, D. Subirá, J. Egido, and A. Ortiz. 2004. Paracetamol-induced renal tubular injury: a role for ER stress. *J. Am. Soc. Nephrol.* 15:380–389. http://dx.doi.org/10.1097/01.ASN.0000111289.91206.B0

Love, K.T., K.P. Mahon, C.G. Levins, K.A. Whitehead, W. Querbes, J.R. Dorkin, J. Qin, W. Cantley, L.L. Qin, T. Racie, et al. 2010. Lipid-like materials for low-dose, in vivo gene silencing. *Proc. Natl. Acad. Sci. USA.* 107:1864–1869. http://dx.doi.org/10.1073/pnas.0910603106

Martinon, F., X. Chen, A.H. Lee, and L.H. Glimcher. 2010. TLR activation of the transcription factor XBP1 regulates innate immune responses in macrophages. *Nat. Immunol.* 11:411–418. http://dx.doi.org/10.1038/ni.1857

Matthews, A.M., D.W. Roberts, J.A. Hinson, and N.R. Pumford. 1996. Acetaminophen-induced hepatotoxicity. Analysis of total covalent binding vs. specific binding to cysteine. *Drug Metab. Dispos.* 24:1192–1196.

McMahon, M., K. Itoh, M. Yamamoto, and J.D. Hayes. 2003. Keap1-dependent proteasomal degradation of transcription factor Nrf2 contributes to the negative regulation of antioxidant response element-driven gene expression. *J. Biol. Chem.* 278:21592–21600. http://dx.doi.org/10.1074/jbc.M300931200

Mitchell, J.R., D.J. Jollow, W.Z. Potter, D.C. Davis, J.R. Gillette, and B.B. Brodie. 1973a. Acetaminophen-induced hepatic necrosis. I. Role of drug metabolism. *J. Pharmacol. Exp. Ther.* 187:185–194.

Mitchell, J.R., D.J. Jollow, W.Z. Potter, J.R. Gillette, and B.B. Brodie. 1973b. Acetaminophen-induced hepatic necrosis. IV. Protective role of glutathione. *J. Pharmacol. Exp. Ther.* 187:211–217.

Mori, K., W. Ma, M.J. Gething, and J. Sambrook. 1993. A transmembrane protein with a cdc2+/CDC28-related kinase activity is required for signaling from the ER to the nucleus. *Cell.* 74:743–756. http://dx.doi.org/10.1016/0092-8674(93)90521-Q

Nagy, G., T. Kardon, L. Wunderlich, A. Szarka, A. Kiss, Z. Schaff, G. Bánhegyi, and J. Mandl. 2007. Acetaminophen induces ER dependent signaling in mouse liver. *Arch. Biochem. Biophys.* 459:273–279. http://dx.doi.org/10.1016/j.abb.2006.11.021

Nakagawa, H., S. Maeda, Y. Hikiba, T. Ohmae, W. Shibata, A. Yanai, K. Sakamoto, K. Ogura, T. Noguchi, M. Karin, et al. 2008. Deletion of apoptosis signal-regulating kinase 1 attenuates acetaminophen-induced liver injury by inhibiting c-Jun N-terminal kinase activation. *Gastroenterology.* 135:1311–1321. http://dx.doi.org/10.1053/j.gastro.2008.07.006

Oikawa, D., M. Tokuda, A. Hosoda, and T. Iwawaki. 2010. Identification of a consensus element recognized and cleaved by IRE1 alpha. *Nucleic Acids Res.* 38:6265–6273. http://dx.doi.org/10.1093/nar/gkq452

Patten, C.J., P.E. Thomas, R.L. Guy, M. Lee, F.J. Gonzalez, F.P. Guengerich, and C.S. Yang. 1993. Cytochrome P450 enzymes involved in acetaminophen activation by rat and human liver microsomes and their kinetics. *Chem. Res. Toxicol.* 6:511–518. http://dx.doi.org/10.1021/tx00034a019

Postic, C., M. Shiota, K.D. Niswender, T.L. Jetton, Y. Chen, J.M. Moates, K.D. Shelton, J. Lindner, A.D. Cherrington, and M.A. Magnuson. 1999. Dual roles for glucokinase in glucose homeostasis as determined by liver and pancreatic beta cell-specific gene knock-outs using Cre recombinase. *J. Biol. Chem.* 274:305–315. http://dx.doi.org/10.1074/jbc.274.1.305

Raucy, J.L., J.M. Lasker, C.S. Lieber, and M. Black. 1989. Acetaminophen activation by human liver cytochromes P450IIE1 and P450IA2. *Arch. Biochem. Biophys.* 271:270–283. http://dx.doi.org/10.1016/0003-9861(89)90278-6

Reimold, A.M., A. Etkin, I. Clauss, A. Perkins, D.S. Friend, J. Zhang, H.F. Horton, A. Scott, S.H. Orkin, M.C. Byrne, et al. 2000. An essential role in liver development for transcription factor XBP-1. *Genes Dev.* 14:152–157.

Reimold, A.M., N.N. Iwakoshi, J. Manis, P. Vallabhajosyula, E. Szomolanyi-Tsuda, E.M. Gravallese, D. Friend, M.J. Grusby, F. Alt, and L.H. Glimcher. 2001. Plasma cell differentiation requires the transcription factor XBP-1. *Nature.* 412:300–307. http://dx.doi.org/10.1038/35085509

Ron, D., and P. Walter. 2007. Signal integration in the endoplasmic reticulum unfolded protein response. *Nat. Rev. Mol. Cell Biol.* 8:519–529. http://dx.doi.org/10.1038/nrm2199

Rutkowski, D.T., and R.S. Hegde. 2010. Regulation of basal cellular physiology by the homeostatic unfolded protein response. *J. Cell Biol.* 189:783–794. http://dx.doi.org/10.1083/jcb.201003138

Thummel, K.E., C.A. Lee, K.L. Kunze, S.D. Nelson, and J.T. Slattery. 1993. Oxidation of acetaminophen to N-acetyl-p-aminobenzoquinone imine by human CYP3A4. *Biochem. Pharmacol.* 45:1563–1569. http://dx.doi.org/10.1016/0006-2952(93)90295-8

Todd, D.J., L.J. McHeyzer-Williams, C. Kowal, A.H. Lee, B.T. Volpe, B. Diamond, M.G. McHeyzer-Williams, and L.H. Glimcher. 2009. XBP1 governs late events in plasma cell differentiation and is not required for antigen-specific memory B cell development. *J. Exp. Med.* 206:2151–2159. http://dx.doi.org/10.1084/jem.20090738

Urano, F., X. Wang, A. Bertolotti, Y. Zhang, P. Chung, H.P. Harding, and D. Ron. 2000. Coupling of stress in the ER to activation of JNK protein kinases by transmembrane protein kinase IRE1. *Science.* 287:664–666. http://dx.doi.org/10.1126/science.287.5453.664

Wang, X.Z., H.P. Harding, Y. Zhang, E.M. Jolicoeur, M. Kuroda, and D. Ron. 1998. Cloning of mammalian Ire1 reveals diversity in the ER stress responses. *EMBO J.* 17:5708–5717. http://dx.doi.org/10.1093/emboj/17.19.5708

Yoshida, H., T. Matsui, A. Yamamoto, T. Okada, and K. Mori. 2001. XBP1 mRNA is induced by ATF6 and spliced by IRE1 in response to ER stress to produce a highly active transcription factor. *Cell.* 107:881–891. http://dx.doi.org/10.1016/S0092-8674(01)00611-0

Zaher, H., J.T. Buters, J.M. Ward, M.K. Bruno, A.M. Lucas, S.T. Stern, S.D. Cohen, and F.J. Gonzalez. 1998. Protection against acetaminophen toxicity in CYP1A2 and CYP2E1 double-null mice. *Toxicol. Appl. Pharmacol.* 152:193–199. http://dx.doi.org/10.1006/taap.1998.8501

Zhang, K., H.N. Wong, B. Song, C.N. Miller, D. Scheuner, and R.J. Kaufman. 2005. The unfolded protein response sensor IRE1alpha is required at 2 distinct steps in B cell lymphopoiesis. *J. Clin. Invest.* 115:268–281.

Zhang, K., S. Wang, J. Malhotra, J.R. Hassler, S.H. Back, G. Wang, L. Chang, W. Xu, H. Miao, R. Leonardi, et al. 2011. The unfolded protein response transducer IRE1α prevents ER stress-induced hepatic steatosis. *EMBO J.* 30:1357–1375. http://dx.doi.org/10.1038/emboj.2011.52